

A Study of Sonic Boom Test with Nozzle Plume Interactions

LI Xuefei^{1,2}, LIU Zhongchen^{1,2}, QIAN Zhansen^{1,2}

¹ AVIC Aerodynamics Research Institute, Shenyang 110034, China

² National Lab. for Computational Fluid Dynamics, School of Aeronautic Science and Engineering

Abstract

The nozzle jet of supersonic aircraft have complex flow disturbance with its aft-body components, and sonic boom prediction under this condition is a problem with highly challenging and high uncertainty. In order to know the influence of jet flow on sonic boom characteristics, CFD method is used to design sonic boom test under nozzle jet conditions and to analyze typical impact factors of sonic boom. The results show that both the two internal geometric schemes of the support can ensure proper flow characteristics of nozzle and jet flow. The difference between the total pressure loss of the two schemes is not large, so the internal flowpath of the support can be determined according to manufacturing difficulties. The reflected wave of the model head shock from the tunnel wall intersects with jet flow at about 15 inches from the exit of the nozzle at Ma number 1.5, which is far upstream compared with the support shock wave interference. Increasing the test Ma number to 2.0 makes the intersection point of the reflected shock wave with the pressure rail move 20 inches downstream, and therefore the final test Ma number is determined to be 2.0 and 2.5. The test scheme is validated and optimized to effectively reduce the number of invalid test and improve the quality of test data.

Keywords: nozzle jet flow; sonic boom; CFD; test; NPR

1. Introduction

The sonic boom is an important obstacle that restricts the real commercial operation of the next-generation supersonic passenger aircraft ^[1,2]. At present, the design of low-sonic boom aircraft at home and abroad has achieved great success ^[3-10], figure 1 shows the next-generation supersonic passenger aircraft that Boeing plans to develop, but the high-precision prediction technology of sonic boom is still the key technology for the new generation of environmental friendly supersonic airliner design, especially the prediction of sonic boom loudness under the condition of complex flow interference and wave structure between the aircraft wake and its aft-body components is still a challenging problem. The interference between the nozzle jet and the aft-body parts of the aircraft is one of the typical influencing factors that affect the uncertainty of the high-precision prediction of the near-field pressure characteristics of the aircraft.



Figure 1 –The Next Generation of Supersonic Transport to Be Developed By Boeing^[3]

From the existing research results, NASA and its industrial partners rely on “The Commercial Supersonic Technology” plan to promote the future development of low sonic boom supersonic civil aircraft technology. Now, research has been carried out on the low sonic boom design scheme to eliminate the influence of jet flow and the influence of intake and exhaust on the prediction of sonic boom ^[11,12]. In China, a series of researches are mainly carried out on the design of low sonic boom supersonic airliner, far-field sonic boom prediction method and sonic boom standard model test ^[13-16]. In 2018, relying on the zero one space flight test platform OS-XO, AVIC Aerodynamics

Research Institute developed the ground measurement technology of sonic boom signal in flight, which is the first publicly successful flight test of the sonic boom characteristics of a supersonic vehicle in China. In recent years, china has established a certain technical foundation and equipment reserves for the three research methods of sonic boom including : numerical simulation, ground test and flight test, but the research on high-precision prediction technology of aircraft sonic boom characteristics in complex flow environment such as intake and exhaust has not been carried out.

The influence of nozzle jet on the sonic boom performance of modern aircraft is related to the scale, position, the intensity of the shock wave of the aircraft afterbody, and the interaction between the wave system and the nozzle jet. A wind tunnel test study is carried out on the effect of nozzle jet sonic boom in the FL-60 wind tunnel of AVIC Aerodynamics Research Institute. The cold high-pressure gas is blown into the blade support, and the gas flows into the axisymmetric nozzle to simulate different nozzle pressure ratio (NPR).The expansion state of the jet is controlled by the nozzle pressure ratio.

Based on the self-developed ARI-OVERSET numerical simulation platform, this paper evaluates and optimizes the wind tunnel test scheme for the sonic boom influence of nozzle jet, understands the complex flow of this kind of complex model, studies the influence of factors such as support interference, NPR, and Ma number , and completes the numerical simulation prediction under a series of test conditions, so as to ensure the validity and economy of the test. The numerical simulation database of this test is established, which is used to compare the CFD results with the test results, and verify the accuracy of CFD solver.

2. Test Equipment and Test Model

Located in Shenyang, FL-60, a 1.2m ×1.2m blow down trisonic wind tunnel with flexible nozzle, is mainly used to test Ma 2.0~4.0 supersonic aircrafts including near space aircraft, aerospace plane, missile etc., besides, industrial test of subsonic, transonic and supersonic aircrafts below M2.0 . The range of Ma number is 0.3 to 4.0. The total operating pressure range of the wind tunnel is 103000-680000Pa, and the Reynolds number range is 7.0-33.8 million per meter.

The key point of the test design is to build a non-interference support to achieve a 20 inch (508 mm) and above pollution-free jet area. It can be seen from Figure 2 and Figure 3 that the intersection position of the reflected head shock wave and the jet is before the shock wave of the support. CFD technology is used to verify the interference position relationship of the above wave system, and master the influence degree of these waves on the pressure signal.

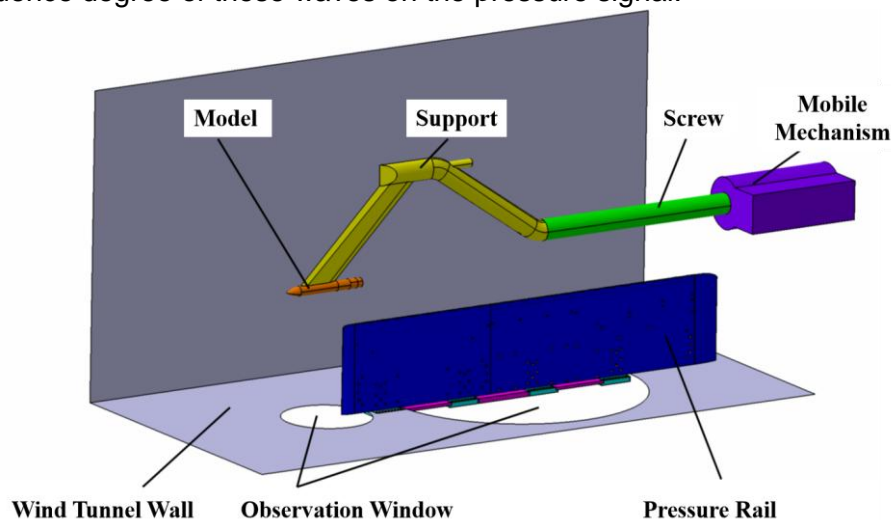


Figure 2 –Model And Pressure Rail Installation Diagram (Axial Rotation 90°).

The throat diameter of the convergent divergent nozzle is 25.56 mm, the nozzle outlet diameter is 33.54 mm, the area ratio is 1.72, and the design point NPR is 8.12. The model is installed laterally. The pressure rail is installed on the side wall of the test section to collect the pressure signal under the model. The pressure tap on top of the pressure rail is 343mm from the wind tunnel wall. The length of the no shock reflection zone is 660.93mm at mach number 1.5 and 996.96mm at mach

number 2.0. The schematic diagram of the test scheme and wave system distribution is shown in Figure 3. The reflected shock wave of the model on the wall facing downstream is represented by a red dotted line. The distance between the model and the top of the pressure rail is controlled by the wind tunnel support, which can move the model horizontally in the test section.

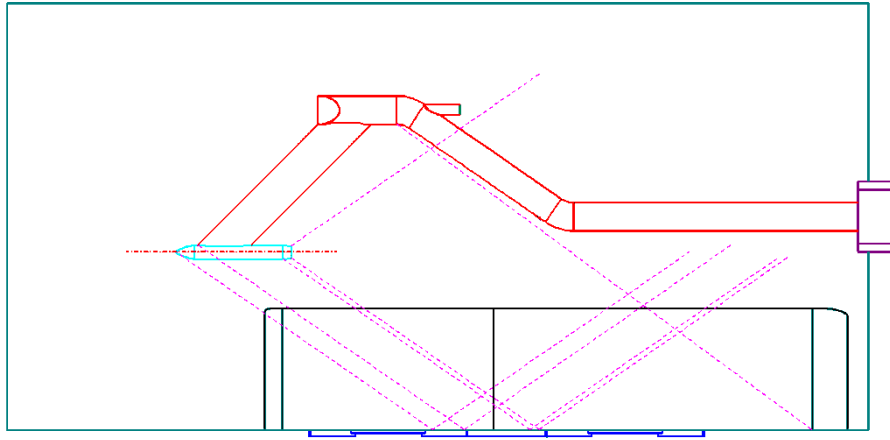


Figure 3 –Test Scheme And Wave System Distribution Diagram.

The planned test Ma numbers are 1.5, 2.0, and 2.5, respectively. The NPR of the test model is controlled at 1, 4, 8, 14 and 20 to simulate jets of different shapes and strengths in the state of no jet, under-expansion and over-expansion. NPR 4, 8, 14 are typical low Ma number nozzle operating conditions.

3. Simulation Method

All calculations in this paper are based on the self-developed ARI-OVERSET numerical simulation platform. ARI-OVERSET can accurately solve complex models, using compressible NS equations and unstructured grids, and has been verified by research to effectively solve supersonic flows^[17]. The grid-centered second-order finite volume discretization method, the SA turbulence model, the convection term adopts the AUSMDV format, and the improved Van_Leer limiter is applied.

This study uses grid generation technology suitable for sonic boom prediction. Figure 4 shows the surface mesh and symmetry surface mesh distribution of the model and the support. In all calculations in this paper, the grid generation is based on the model located in the free incoming flow, because research shows that the free incoming flow simulation can reliably reproduce the wind tunnel test pressure data.

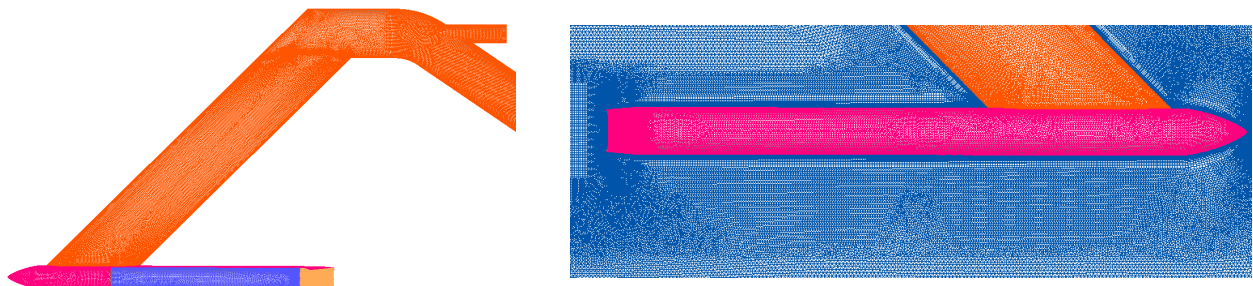


Figure 4 –Mesh Distribution of Test Model And Support.

The whole flow path of high pressure gas through flexible pipe, support and nozzle is very complicated. The mass flow rate and total pressure loss upstream of the system are unpredictable. In the design stage of the inner channel of the test system, the whole inner channel simulation method is adopted, that is, the inlet boundary condition is set at the top of the support (see Figure 3 green solid line section of the support), and the total temperature and total pressure are given. The initial total pressure value is given by predicting the total pressure loss of the flow path. After the total pressure loss of the internal flow path is determined by several numerical simulation tests, the total pressure condition of the inlet is given according to the total pressure of the nozzle inlet plus the total pressure loss of the internal flow path, and the total pressure of the nozzle inlet is determined according to the nozzle pressure ratio. The total temperature is given based on wind tunnel conditions. Another method similar to this is to set the inlet plane at a certain section in front

of the internal contraction section of the nozzle, and give the total temperature and pressure conditions. According to $P_{TN} = NPR * P$, the total pressure P_{TN} is determined by the nozzle pressure ratio NPR and static pressure P of the free flow, and the total temperature is also given based on the wind tunnel conditions. This approximation does not take into account the non-uniformity of flow, such as the non-uniformity caused by the boundary layer of nozzle and the flow direction change from support to nozzle. However, the CFD method can obtain the preliminary evaluation results of shock jet interference with sufficient accuracy under a wide range of flow conditions. Therefore, this setting is used in all calculations except the design of inner flow channel and the evaluation of the influence of inner flow path on jet. All calculation conditions are given in Table 1.

Table 1 –Calculation Conditions.

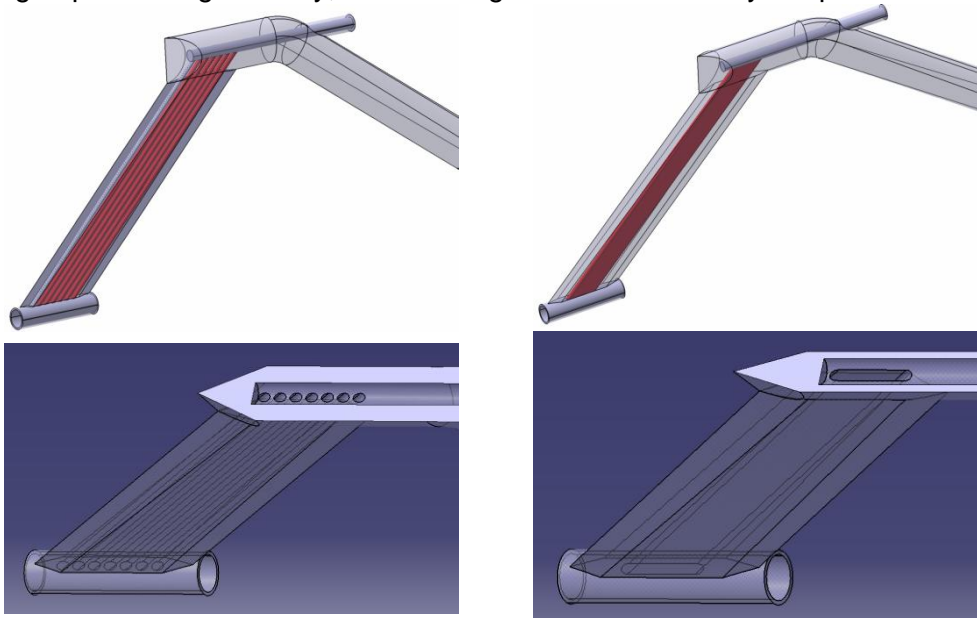
Mach number	Model	NPR
1.5/2.0/2.5	Model	4/8/14/20
1.5/2.0/2.5	Model +Support	4/8/14/20
1.5/2.0/2.5	Lengthened model	1/4/8/14/20
1.5/2.0/2.5	Lengthened model+ Support	1/4/8/14/20

The NPR here is defined as follows: the ratio of the total pressure at the inlet to the free flow pressure. By changing the nozzle pressure ratio from no flow (NPR = 1) to under expansion (NPR = 20), the nozzle jets with no jet (NPR = 1), strong under expansion (NPR = 20), weak under expansion (NPR = 14), near complete expansion (NPR = 8) and over expansion (NPR = 4) were compared.

4. Test Design Based on CFD

Before the test, CFD technology is used to verify the rationality of the test scheme, and to assist the optimization design of flow path and support system of the model. In the initial stage of the design, the internal flow path design is carried out to understand the flow details in the support and the jet, so as to ensure that the flow have appropriate flow characteristics.

The actual internal flow path of the high-pressure jet is very narrow, and it is connected to the nozzle through the blade support, and the connection angle is 45 degrees. Figure 5 shows the seven-tube and single tube design scheme of the internal flow path design of high pressure jet support referring to the red object surface, and a cross-sectional view of the cross arm is shown below to assist in observing the internal structure. The design goal of the internal flow path of the jet is to form a flow throat at the throat of the nozzle, so as to ensure the uniformity of the jet and the consistency of the mass flow rate. The research results show that both of the two schemes can achieve the design goals, and the total pressure loss is not much different. It can be selected according to processing difficulty, and the single tube one is finally adopted.



(a) Seven tube scheme

(b) One tube scheme

Figure 5 –Internal Flow Path Design of High Pressure Jet Support.

The initial planned test Ma numbers are 1.5, 2.0 and 2.5, but the simulation results show that at Ma1.5, the shock wave of the model head is reflected by the tunnel wall and intersects with the jet about 15 inches away from the nozzle. At this Ma number, the impact of the reflected head shock on the jet area is far upstream compared with the support shock interference, and the head shock reflection pollution area accounts for a large proportion. The distance between the head shock wave and the jet pollution zone is consistent for all model heights. Therefore, it is necessary to use a larger test Ma number to make the reflected wave of the model head shock move downstream to reduce its influence.

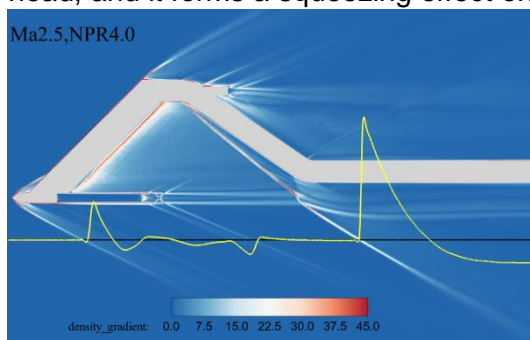
Increasing the test Ma number to 2.0 makes the intersection of the reflected shock wave and the pressure rail move an additional 20 inches downstream, thus the proportion of pressure pollution areas is reduced effectively. The boundary layer in this simulation is smaller than that in the test, because the simulation model is located in the free flow, and the wall effect is not considered. Therefore, the test reflected wave is more upstream than the predicted value of this simulation. According to the simulation results, it is found that the Ma2.0 and Ma2.5 test conditions are more suitable. If there is no CFD simulation, the test is carried out under Ma1.5 working condition, which will produce a lot of invalid data.

5. Discussion of Results

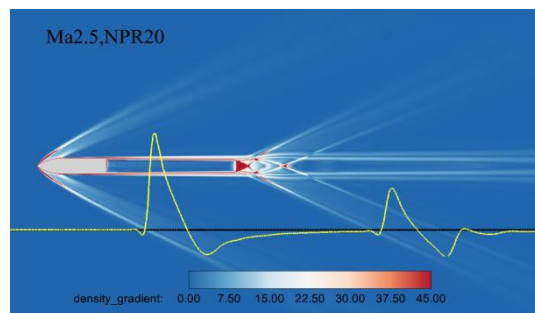
Before the test, CFD technology is applied to extensively verify the validity of the test data. In the design phase of the test model, CFD numerical simulation is carried out on the planned test conditions. The study finds the test data is sensitive to the change of the model length, and it increases by 200 mm has a significant effect on suppressing support interference during the pressure platform before the nozzle jet flow, and hence it should be increased as much as possible within the limits of the tunnel adjustment. After the nozzle length range is determined, the internal flow research is carried out to understand the flow details in the support and the jet, so as to ensure that the flow in the nozzle and the tail jet have appropriate flow characteristics. Then the effects of NPR, Ma number and support interference are determined by CFD. These pre-test simulations help determine the test times, thus reducing the number of invalid test caused by wind tunnel conditions, test conditions and measuring equipment.

5.1 Flow Field

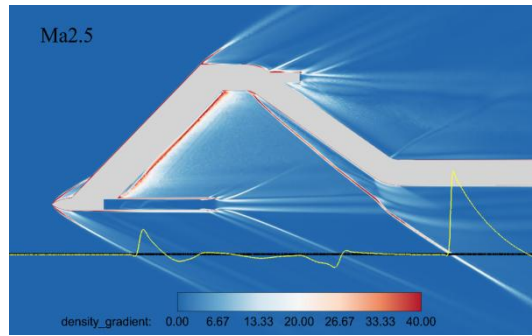
Figure 6 shows the flow field (density gradient) on the symmetry plane and the overpressure distribution at the pressure rail under typical working conditions. The black solid line indicates the measurement position of the pressure rail, and the yellow solid line indicates the overpressure distribution. Figure 7 shows the distribution of Ma number in the symmetric plane when Ma number is 2.5. It can be seen that the shock wave intensity of the support is much higher than that of the model head, and it forms a squeezing effect on the jet, which changes the jet direction and velocity.



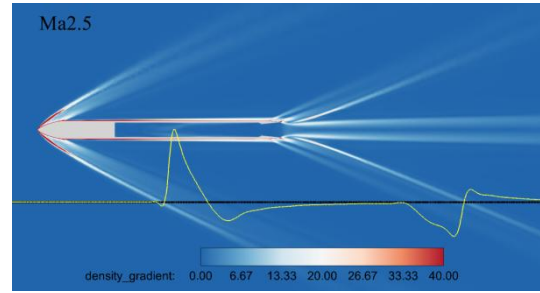
(a) Ma2.5, NPR=4.0



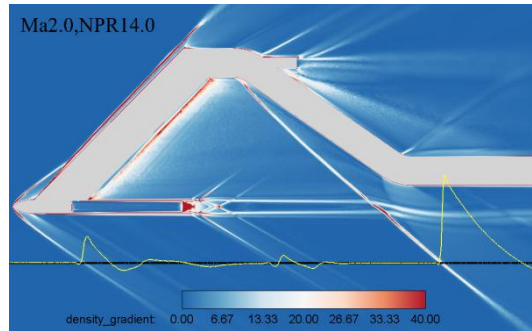
(b) Ma2.5, NPR=20.0



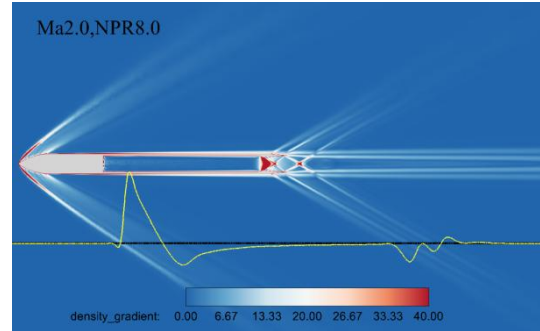
(c) Ma2.5, NPR=1.0



(d) Ma2.5, NPR=1.0

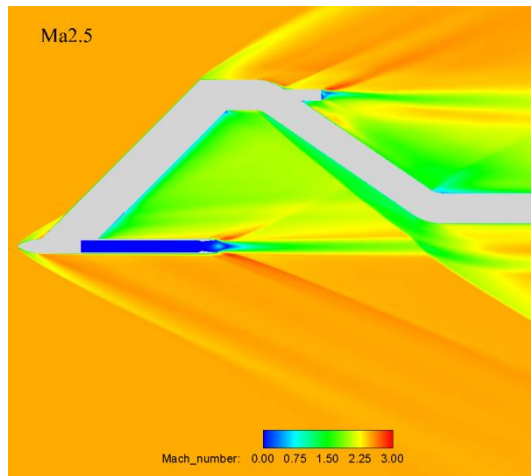


(e) Ma2.0, NPR=14.0

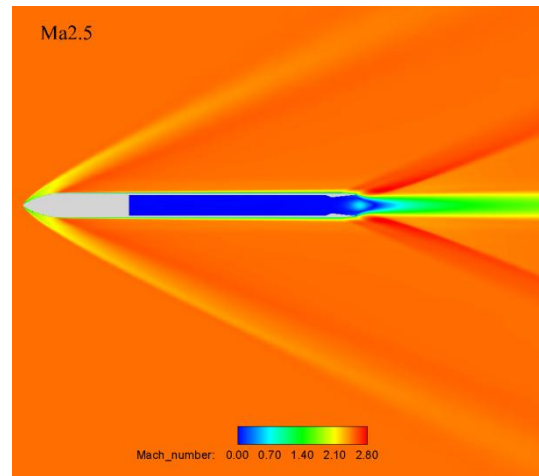


(f) Ma2.0, NPR=8.0

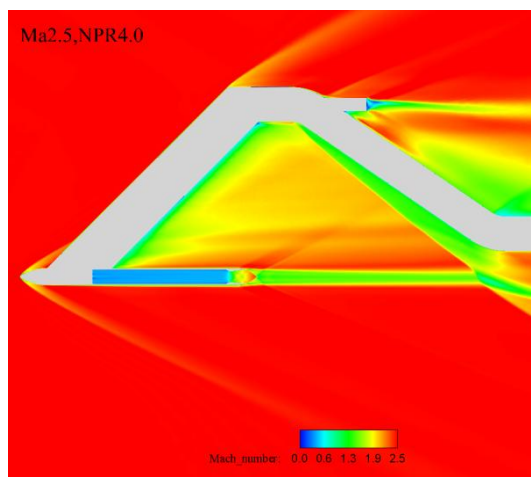
Figure 6 – Density Gradient on the Symmetrical Plane And Overpressure Distribution at Pressure Rail under Typical Conditions



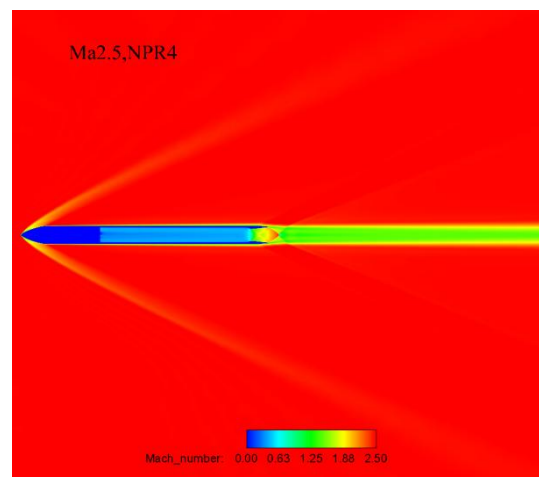
(a) NPR=1.0, With support



(b) NPR=1.0, Without support



(c) NPR=4.0, With support



(d) NPR=4.0, Without support

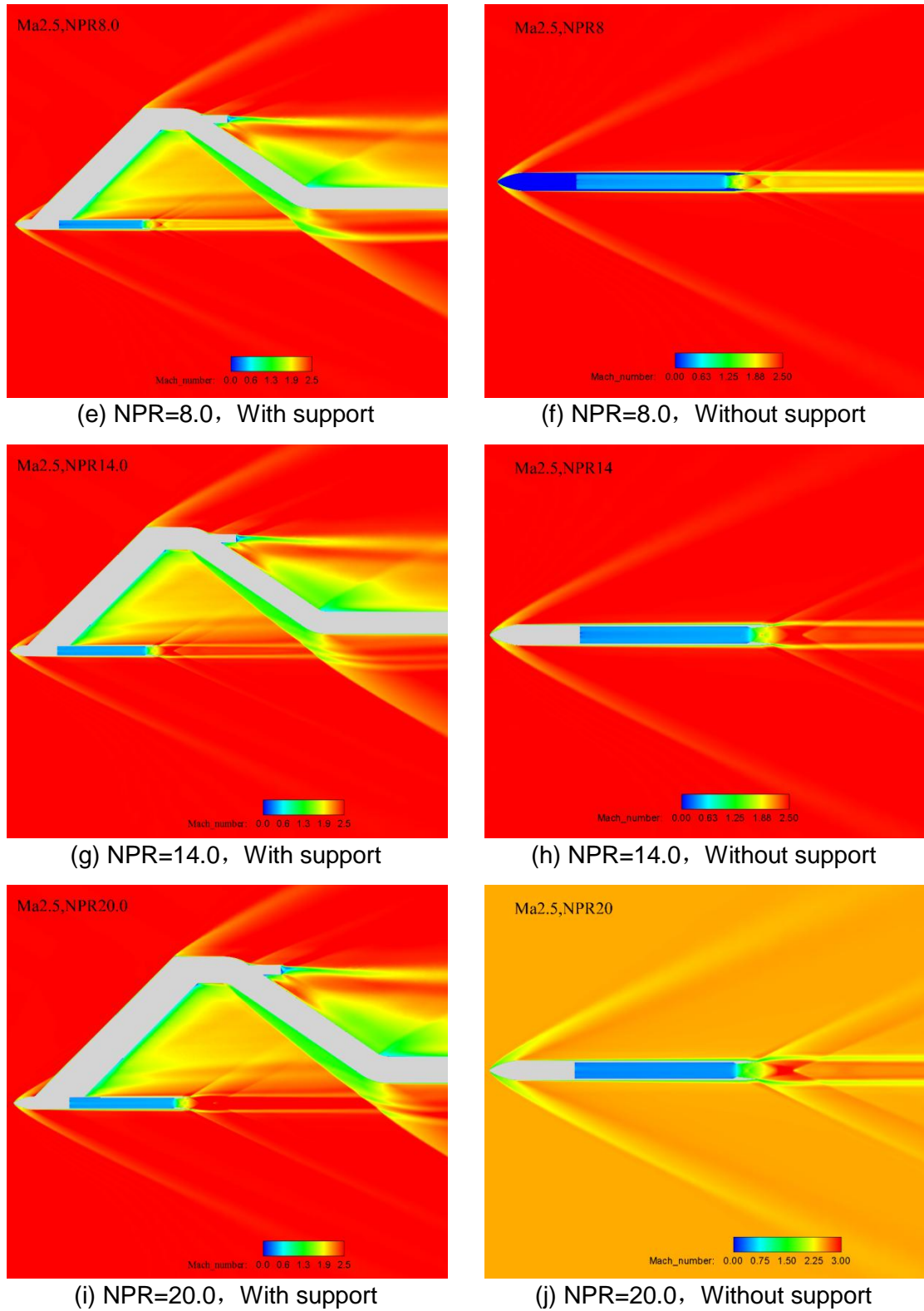


Figure 7 – Ma Number Distribution on the Symmetry Plane at Ma 2.5

Figure 8 shows nozzle jet wave structure with NPR of 4.0 and 14.0 at Ma = 2.0 under typical over expansion and under expansion conditions, using Ma number coloring. The black solid line represents oblique shock, the yellow solid line represents normal shock wave, the green dotted line represents jet boundary, the white dotted line represents expansion wave, the black dotted line represents compression wave, and the purple dotted line represents slip line.

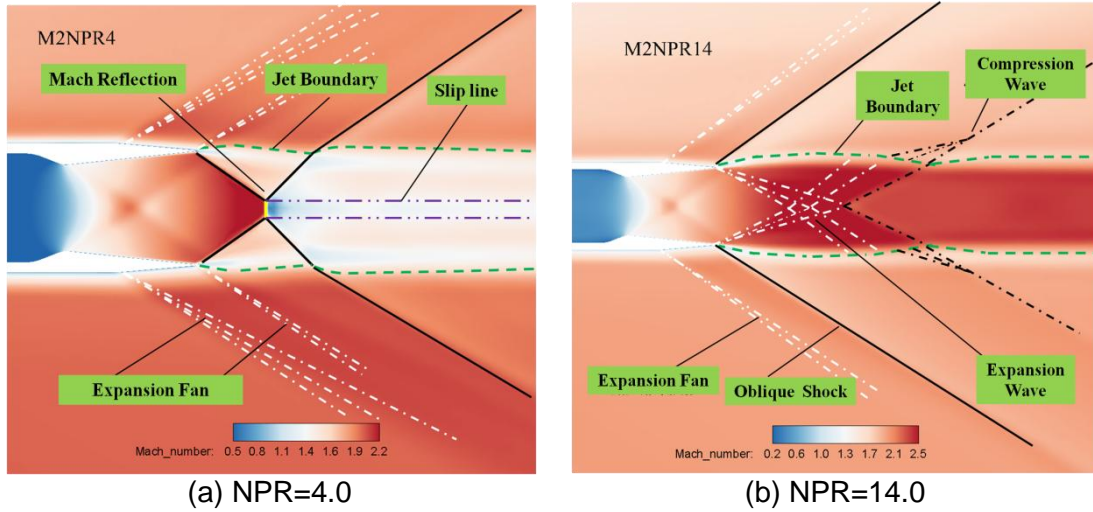
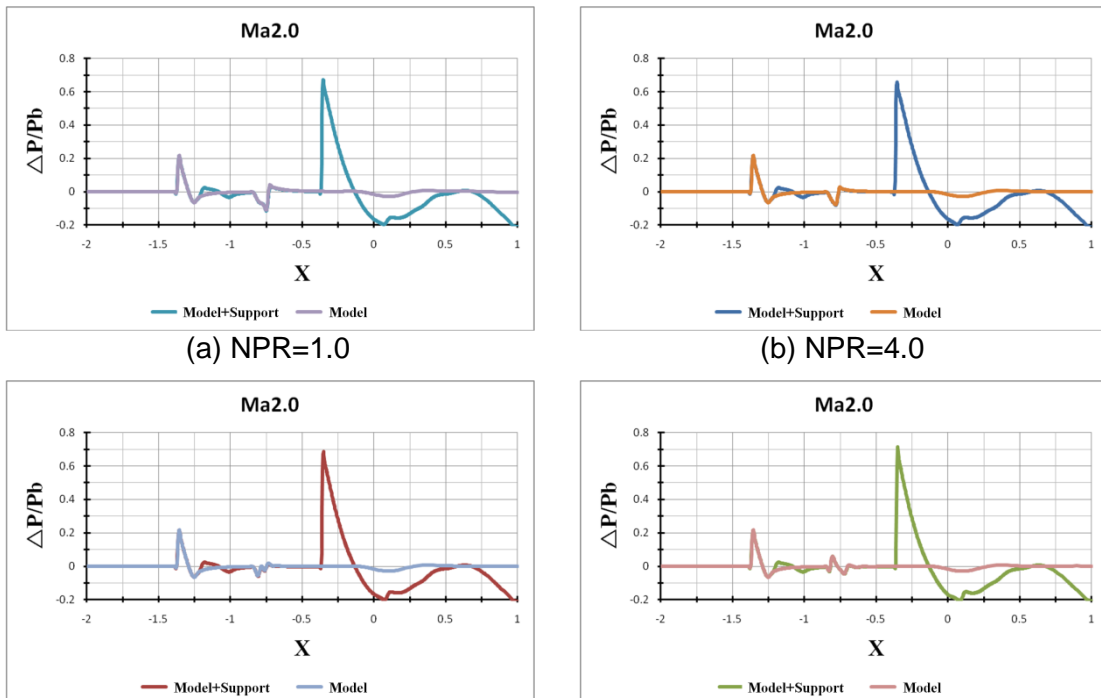


Figure 8 –Typical Jet Wave Structure

When $NPR = 4.0$, the nozzle works in the state of over expansion, the shock wave at the nozzle lip intersects at the axis to form Mach reflection, the reflected shock wave propagates through the jet boundary to the far field, and two slip lines are formed at the three intersection points of Mach reflection. An expansion fan is emitted from the nozzle lip. When $NPR=14.0$, the nozzle works in an under-expanded state, and the lip expansion wave beam intersects the jet boundary and forms a weakly compressed wave beam, and the wave system propagates to the jet outside at the turning point of the curved jet boundary and the direct one. The trailing edge of the nozzle cowl emits a plume shock wave. There is a shear layer between the free flow and the nozzle exhaust flow.

5.2 Support Interference

The influence of support interference under various NPR conditions at mach number 2.0 is analyzed for the extended test model, as shown in Figure 9. It can be seen that the support has no effect on the shock wave of the model head. Under all NPR conditions, the shock wave waveform, shock wave intensity and shock position of the model head are highly consistent, but the support interferes with the pressure platform area in front of the jet, which makes the pressure fluctuation in the platform area. However, the pressure platform area recovers before the wave system induced by the nozzle, which basically has no effect on the jet wave system (the jet wave system is located at about $x = -0.85 \sim -0.75$). The above results show that the wave system of the jet area under the support is in good agreement with that without the support, which indicates that the support design is very successful.



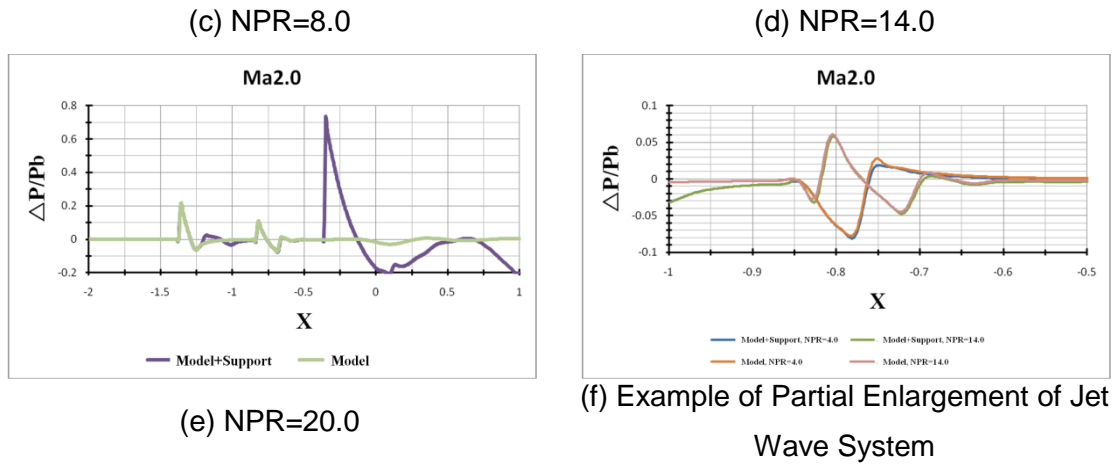


Figure 9 –Extended Model Support Interference at Ma2.0.

5.3 NPR Effect

Nozzle pressure ratio is one of the important parameters affecting jet shape and velocity, so it is very important to accurately predict the influence of NPR change on flow. Figures 10-13 show the pressure signals of the lengthened model with and without support under various NPR conditions, and Figure 14 shows the density gradient distribution of the jet flow near the nozzle. The results show that the waveforms and intensities of the model head shock wave, the expansion wave from cone to cylinder and the support shock wave are completely consistent with each other, which shows that the calculation method adopted is effective and accurate, and the grid generation strategy adopted is suitable for the grid scale, which can reflect the real near-field pressure characteristics for different models.

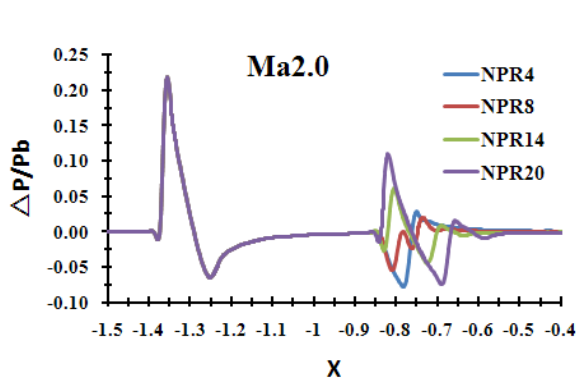


Figure 10 –Pressure Characteristics of the Extended Model with NPR at Ma2.0.

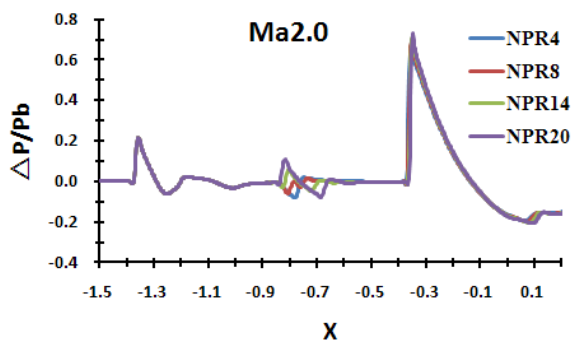


Figure 12 –Pressure Characteristics of the Extended Model And the Support with NPR at Ma2.0.

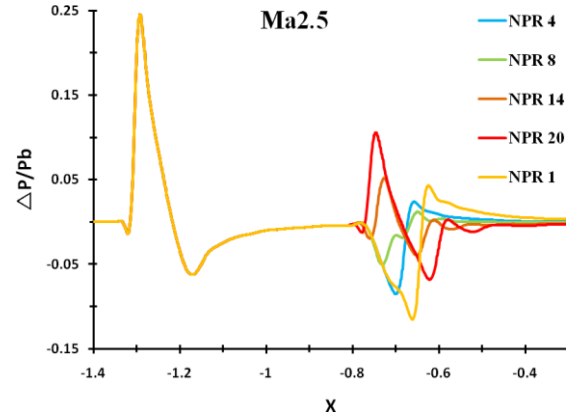


Figure 11 –Pressure Characteristics of the Extended Model with NPR at Ma2.5.

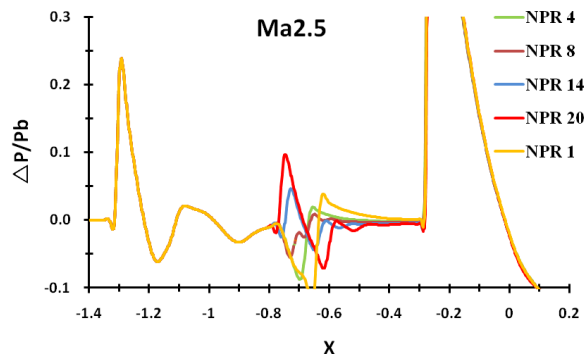


Figure 13 –Pressure Characteristics of the Extended Model And the Support with NPR at Ma2.5.

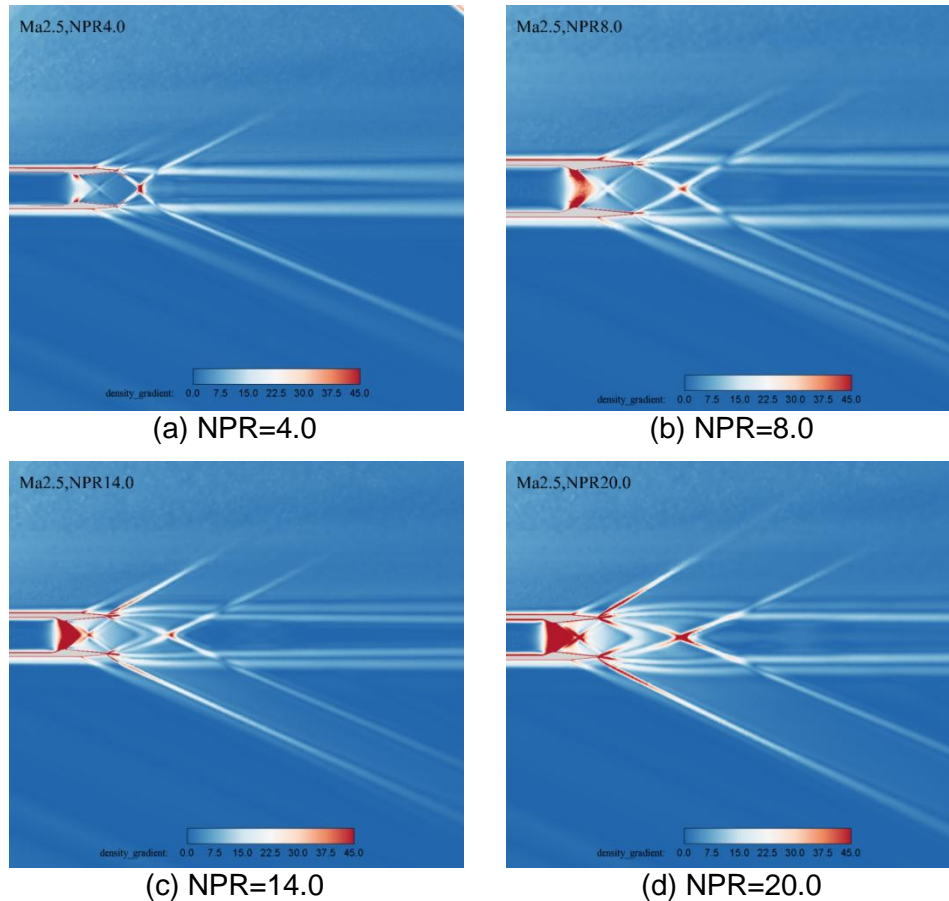


Figure 14 –Density Gradient Distribution of test Model And the Support on the Symmetry Plane.

When $\text{NPR}=1$, there is no nozzle jet, and the "jet" only has a wake behind the nozzle. At this time, the wake is very narrow because the free flow has a squeezing effect on the wake. When $\text{NPR}=4$, the nozzle is in an over-expansion state, an oblique shock wave appears at the lip of the nozzle trailing edge, and a normal shock wave, namely Mach stem, is formed about a diameter from the nozzle outlet. When $\text{NPR}=8$, the nozzle is in a slightly over-expanded state, so the oblique shock wave at the trailing edge of the nozzle intersects further downstream of the jet, and no normal shock wave is generated. When $\text{NPR}=14$ and $\text{NPR}=20$, the nozzle is in an under-expanded state, and an expansion fan is formed at the nozzle outlet lip. Before the shock wave formed by compression and refraction propagates to the jet, the expansion fan reflects at the center line and reaches the jet boundary again.

The jet diameter increases with the increase of NPR. Under all NPR conditions, a clear shock structure can be captured. With the increase of NPR, the shock intensity and length increase. Under all NPR conditions, a clear expansion fan propagating downstream can be observed at the beginning of the boat tail angle, because it is located on the outer wall of the nozzle and has nothing to do with the flow inside the nozzle, so it is basically not affected by NPR.

5.4 Ma Number Effect

Figures 15 to 18 show the variation of the pressure signals at the pressure rail with the Ma number under the two limit states of $\text{NPR}=20$ and $\text{NPR}=1$ for the extended models with and without support. With the increase of Ma number, the wave systems of the two models with or without jet flow move downstream. The shock intensity of the model head shock wave and the support shock wave increases with the increase of Ma number, but the jet waveform and intensity are not affected by Ma number, so it also shows that the model head shock wave and the support shock wave basically do not contaminate the jet flow field, and the design of the test scheme is reasonable.

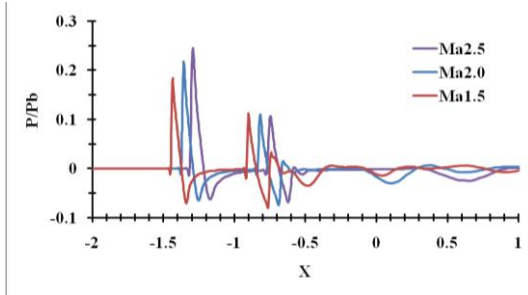


Figure 15 –Overpressure Distribution of Extended Model under NPR=20 Condition

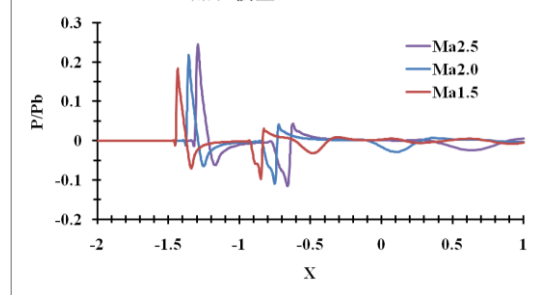


Figure 16 –Overpressure Distribution of Extended Model under NPR=1 Condition

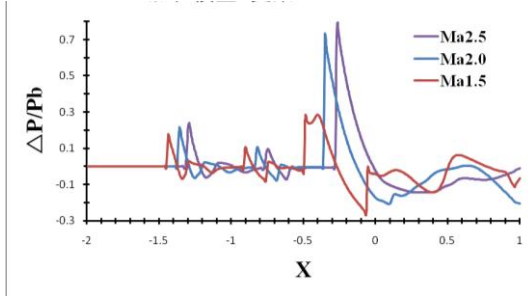


Figure 17 –Overpressure Distribution of Extended Model And the Surport under NPR=20 Condition

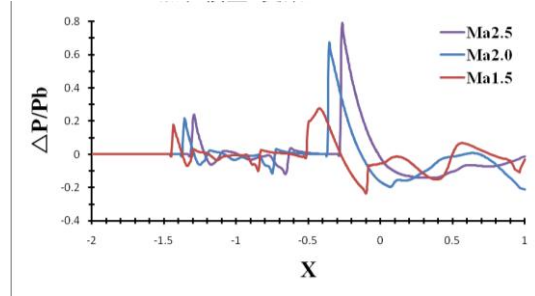


Figure 18 –Overpressure Distribution of Extended Model And the Surport under NPR=1 Condition

6. Conclusion

Based on the self-developed ARI-OVERSET numerical simulation platform, this paper evaluates and optimizes the wind tunnel test for the impact of the nozzle jet sonic boom. Considering the influence of support interference, NPR, Ma number and other factors, the numerical simulation is completed under a series of test conditions. The results show that:

- 1) Based on the CFD method, this paper completes the test scheme design and the optimization design of the test internal flow path, and determines that the flow in the nozzle and the nozzle jet have the target flow characteristics.
- 2) The numerical simulation study before the test reduces invalid tests caused by wind tunnel conditions, test conditions and measuring equipment, ensures the validity of test data and the test economy, and establishes the numerical simulation database of nozzle jet sonic boom effect test. The ICAS conference is postponed due to the impact of Corona Virus Disease 2019 (COVID-19), and so that the relevant tests have been completed before this paper published. The test results are highly consistent with the numerical simulation results of this paper. The relevant research can be found in the related papers to be published by our team.
- 3) The test Mach number determines the scale of the pollution area of the jet contaminated by the reflected wave of the model head shock wave, and it needs to be carefully selected.
- 4) Through the flow field structure around and downstream of the model, the sources of shock wave and expansion wave are determined, the jet shape and boundary are defined, and the influence of jet with the change of incoming flow and afterbody wave system is mastered. The pressure signals further indicate the positions of shock wave and expansion wave in the near field, and the interaction between near-field jet and wave system is analyzed qualitatively and quantitatively.

7. Contact Author Email Address

The contact author email address: 1034774512 @qq.com

8. Copyright Statement

The authors confirm that they, and/or their company or organization, hold copyright on all of the original material included in this paper. The authors also confirm that they have obtained permission, from the copyright holder of any third party material included in this paper, to publish it as part of their paper. The authors confirm that they give permission, or have obtained permission from the copyright holder of this paper, for the publication and distribution of this paper as part of the ICAS proceedings or as individual off-prints from the proceedings.

References

- [1] Morgenstern, J., Norstrud, N., Sokhey J., Martens, S., and Alonso, J., "Advanced Concept Studies for Supersonic Commercial Transports Entering Service in the 2018 to 2020 Period", Phase I Final Report, NASA/CR—2013-217820, February 2013.
- [2] Morgenstern, J., "Final Report for the NASA N+2 Supersonic Validations Phase II: Advanced Concepts Studies for Supersonic Commercial Transports Entering Service in the 2018 to 2020 Period", NASA/CR—2013-X, 2013. Report not yet published.
- [3] Welge H R, Nelson C, Bonet J. Supersonic vehicle systems for the 2020 to 2035 timeframe [R]. AIAA-2010-4930.
- [4] Magee T E, Shaw S G, Fugal S R. Experimental validations of a low-boom aircraft design, AIAA-2013-0646[R]. Reston: AIAA, 2013.
- [5] Yamashita R, Suzuki K. Full-field sonic boom simulation in real atmosphere[R]. AIAA-2014-2269, 2014.
- [6] Rallabhandi S K. Advanced sonic boom prediction using the augmented Burgers equation[J]. Journal of Aircraft, 2011, 48(4): 1245-1253.
- [7] Takeno J, Misaka T, Shimoyama K, et al. Analysis of sonic boom propagation based on the KZK equation[R]. AIAA-2015-0745, 2015.
- [8] ZHU Ziqiang LAN Shilong, Study of supersonic commercial transport and reduction of sonic boom, [J]. Acta Aeronautica et Astronautica Sinica, 2015, 36(08): 2507-2528.
- [9] FENG Xiaoqiang, LI Zhanke SONG, Bifeng, et al. Optimization of sonic boom and aerodynamic based on structured/unstructured hybrid grid[J], Acta Aerodynamica Sinica, 2014, 32(1): 30-37
- [10] FENG Xiaoqiang, Research on Sonic Boom Computation Method and Its Application in Supersonic Commercial Transport Design[D]. Northwestern Polytechnical University, 2012: 9-15.
- [11] Smith, Nathaniel T., Durston, Donald A., and Heineck, James T., "Retroreflective Background Oriented Schlieren Imaging Results from the NASA Plume/Shock Interaction Test," Scitech 2017, 55th AIAA Aerospace Sciences Meeting, AIAA-2017-0043
- [12] Durston, D., Cliff, S., Denison, M., Smith, N., Heineck, J., Kushner, L., Castner, R., Elmilgui, A., Carter, M., Winski, C., Shea, P. and Blumenthal, B., "Nozzle Plume/Shock Interaction Sonic Boom Test Results from the NASA Ames 9- by 7-Foot Supersonic Wind Tunnel", Scitech 2017, 55th AIAA Aerospace Sciences Meeting, AIAA-2017-0041. 25Housman, Jeffrey A., Sozer, Emre, and Kiris, Cetin C., "LAVA Simulations for the First AIAA Sonic
- [13] XU Yue SONG Wanqiang, Near Field Sonic Boom Calculation on Typical LSB Configurations[J]. Aeronautical Science & Technology, 2016, 27(7): 12-16.
- [14] Feng X-Q, Li Z-K, Song B-F. Research of low boom and low drag supersonic aircraft design[J]. Chinese Journal of Aeronautics, 2014, 27(3): 531-541.
- [15] WANG Gang MA Boping LEI Zhijin, et al. Simulation and analysis for sonic boom on several benchmark cases[J]. Acta Aeronautica et Astronautica Sinica, 2018, 39(1): 164-176.
- [16] Ma Boping Wang Gang Lei Zhijin, et al. Numerical Investigation of Influence of Mesh Property in Nearfield Sonic Boom Prediction[J]. Journal of Northwestern Polytechnical University, 2018, 36(5): 865-874.
- [17] Li Xuefei, Liu Yuan and Qian Zhansena, Numerical Simulation Study on SERN Flow In Acceleration/Deceleration Process of High Mach Number Aircraft, The 2016 Asia-Pacific International Symposium on Aerospace Technology, September 16, 2016